

Design and synthesis of *trans* 2-(furan-2-yl)vinyl heteroaromatic iodides with antitumour activity

Cosimo Gianluca Fortuna,^{a,*} Vincenza Barresi,^a Giuliano Berellini^b
and Giuseppe Musumarra^{a,*}

^a*Dipartimento di Scienze Chimiche, Università di Catania, Viale A. Doria, 6, 95125 Catania, Italy*

^b*Laboratorio di Chemiometria e Chemioinformatica, Dipartimento di Chimica, Università degli Studi di Perugia, Via Elce di Sotto, 8, 06100 Perugia, Italy*

Received 1 October 2007; revised 14 December 2007; accepted 20 December 2007

Available online 25 December 2007

Abstract—A new molecular modelling approach based on physico-chemical and pharmacokinetic properties, called Volsurf plus, was used to design new heterocyclic compounds with antiproliferative activity. The synthesis and in vitro antitumour tests on a breast carcinoma cell line (MCF7) confirmed VOLSURF predicted activity values.

© 2008 Elsevier Ltd. All rights reserved.

1. Introduction

Previous work on the design, the synthesis and the antitumour activity of new *trans* 1-heteroaryl-2-(1,3-dimethylimidazolium-2-yl) ethylenes¹ confirmed the hypothesis, based on a Molecular Interaction Field (MIF)^{2,3} approach using Grid-Independent Descriptors GRIND,⁴ that the presence of three aromatic moieties and of halogen atoms are the main structural features necessary to obtain satisfactory antiproliferative activities. The synthesis, QSAR modelling and biological^{5–8} assay of vinyl and halo-furan derivatives has been reported and their activities as antibacterials and anticancer drugs evaluated together with their toxicity effects.^{9–12} Following these leads, we here report the design of new *trans* 2-(furan-2-yl)vinyl heteroaromatic iodides, with pyridinium, imidazolium and quinolinium as ethylene-linked heteroaromatic cations and halo substituted benzenes in the 5-position of the furan ring, with the aim to optimize the antitumour activities. It is well known that an increased drug–receptor interaction does not necessarily imply an increase in biological activity. Therefore, it is also very important to design new structures which exhibit ADME (Adsorption, Distribution, Metabolism, and Elimination) properties warranting an acceptable bio-

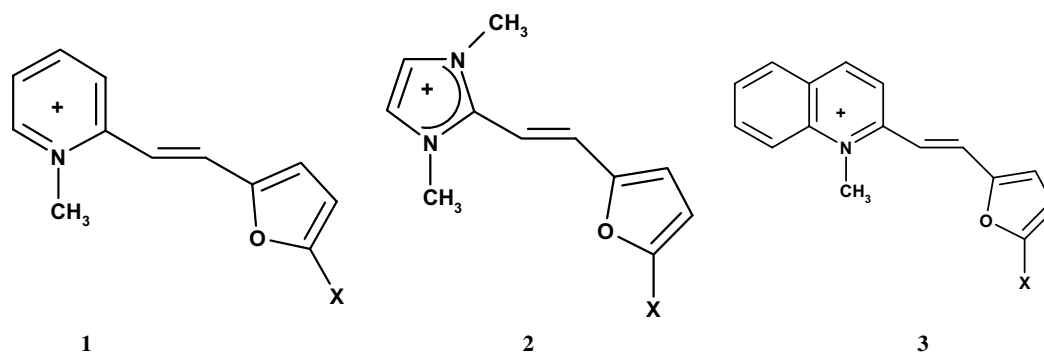
availability. Very simple heuristic rules concerning cutoffs on molecular weight, number of hydrogen bond donor/acceptors and lipophilicity only represent crude guidelines working well at the lead-finding stage, but less suitable to establish structure–property relationships in lead optimization.¹³ Other frequently used descriptor schemes are topological indices, but their interpretation in terms of molecular structures is not straightforward. In the present work, a high-throughput chemoinformatic approach, called Volsurf plus, including both modelling of ADME properties in the design of new structures and the correlation 3D molecular fields with physico-chemical and pharmacokinetic properties, will be adopted for predicting the in vitro antitumour activity of these new compounds. The structural modifications suggested by the above molecular modelling approach will be verified by the synthesis of the designed molecules and their activity evaluation tests.

2. Results and discussion

The structures of compounds previously synthesized and of new compounds are reported in [Scheme 1](#). Ten structures previously modelled using a program called Almond based on a structural classification were selected to derive another model by a novel methodology called Volsurf plus. Volsurf is an automatic procedure to convert 3D molecular fields into physico-chemically relevant molecular descriptors. In the standard procedure,

Keywords: Molecular modelling; Antitumour compounds; Heterocycles; QSAR.

* Corresponding authors. Tel.: +39 0957385004; fax: +39 095580138; e-mail: cg.fortuna@unict.it



X	Designation
H	a
Methyl	b
Bromo	c
2-Chlorophenyl	d
3-Chlorophenyl	e
4-Chlorophenyl	f
4-Bromophenyl	g
2,5-Dichlorophenyl	h
2,4-Dichlorophenyl	i
3,4-Dichlorophenyl	j
3-Chloro-4-methoxyphenyl	k
4-Chloro-2-nitrophenyl	l
2-Chloro-5-(trifluoromethyl)-phenyl	m

Scheme 1. Structure of 2-(furan-2-yl) vinyl-heteroaromatic iodides.

the interaction fields with a water probe and a hydrophobic probe are calculated for all molecules in the dataset. The basic concept of Volsurf is to extract the information present in 3D molecular field maps into few quantitative numerical descriptors, which are easy to understand and interpret. Molecular recognition is achieved using image analysis software coupled with external chemical knowledge. Within this context Volsurf selects the most appropriate descriptors and parameterization according to the type of 3D maps under study. The molecular descriptors obtained refer to molecular size and shape, to size and shape of both hydrophilic and hydrophobic regions and to the balance between them. Hydrogen bonding, amphiphilic moments and critical packing parameters are other useful descriptors. The Volsurf descriptors are presented and explained in detail in Section 3. The originality of Volsurf resides in the fact that surfaces, volumes and other related descriptors can be directly obtained from 3D molecular fields with simple computational algorithms. Moreover, Volsurf descriptors can be easily obtained for small, medium and large molecules, as well as for biopolymers such as DNA sequences, peptides and proteins. No parameterization is required and the descriptors can be used for multivariate model building to correlate the 3D molecular structures with biological behaviour.¹⁴ The VolSurf methodology can also be applied for structure-activity relationships and molecular diversity based on surface properties. The computational procedure is fully automated and quite fast. The ten structures present in the first model, test set, contain a differently substituted furan ring linked by an ethylenic bond to an imidazolium or pyridinium salt, apart from one structure with a furan ring between two vinylpyridinium salts (**PF**₂) already selected for comparison

because it is among the most active compounds previously synthesized by our group.¹⁵ The code number and the antiproliferative in vitro activities for the ten compounds chosen as test set are reported in Table 1. The 3D structures of compounds (**1c**, **1d**, **1g**, **2a–d**, **2g**) and for 2,6-di-[2-(furan-2-yl)vinyl]pyridinium iodide (**PF**₂) were imported, in Mol-file, and coded as VOL-SURF descriptors following the procedure described in Section 3.1.

This new methodology offers a new tool, called Volsurf plus designer, that makes us able to design new compounds and to project them on our test set model. Structural modifications in the design of new structures, with the aim to improve the antitumour activities, consisted in the insertion of new substituents on the benzene linked in the 5-position of the furan ring and introducing a new salt as the quinolinium one. The scores plot projection provided guidelines in the selection of new structures to be synthesised. In Figure 1 the scores plot with the ten structures of the test set

Table 1. Activity values for compounds in the test set

Compound	LogGI ₅₀ (μM)
1a	−4.15
1c	−5.10
1d	−5.65
1g	−6.00
2a	−4.00
2b	−4.48
2c	−4.40
2d	−5.86
2g	−6.21
PF ₂	−5.60

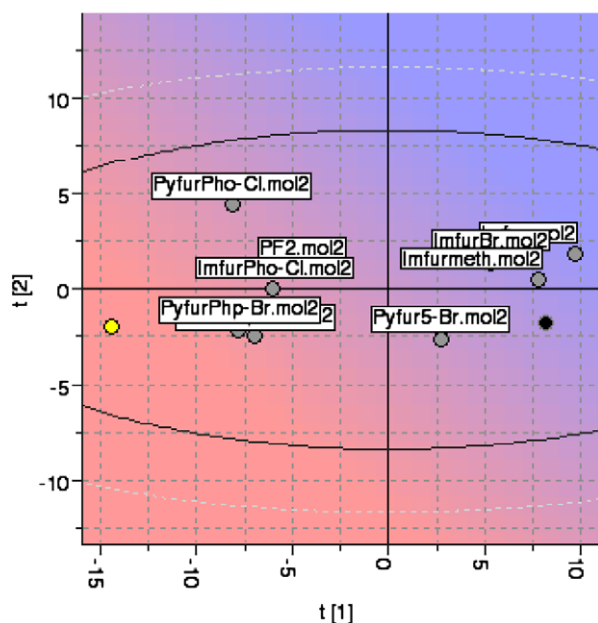


Figure 1. Scores plot of the test set and of the new structure 3f.

Table 2. Predicted activity values for the designed compounds

Compound	Predicted activity values
3c	-5.57
2e	-5.84
3l	-6.31
2f	-5.56
1j	-6.23
1m	-5.65
2k	-5.52
1f	-5.92
2h	-6.14
3k	-6.40
1e	-5.93
3f	-6.70
1i	-6.24
1k	-5.66
3e	-6.64
1h	-6.18

and one of the new compounds are reported as an example. The background was coloured according to the activity values; the red zone indicates the higher activity and the yellow point is the new structure. It is possible to see that the predicted activity of 3f is higher than those of the compounds previously published. In Table 2 the predicted activities for 16 new structures are reported.

To verify the above hypothesis we proceeded with the synthesis and in vitro biological evaluation of the above derivatives. The synthesis of *trans* 2-(furan-2-yl)vinyl heteroaromatic iodides can be achieved by condensation of imidazolium, piridinium or quinolini-

um iodides with heteroaromatic aldehydes in the presence of NaOH (see Section 3), exploiting the acidity of the above salts' α methyls due to the electron-withdrawing effect of the adjacent positively charged ring nitrogens.

Under appropriate experimental conditions pure *trans* isomers were obtained, as evidenced by the ethylenic protons' *J* coupling constants in the NMR spectra.

The anti-proliferative activity of all the newly synthesized compounds was then tested against a tumour cell line, breast carcinoma (MCF7). The in vitro activities, expressed as log GI₅₀ values (see Section 3), are recorded in Table 3, together with that of 2,6-di-[2-(furan-2-yl)vinyl]pyridinium iodide (PF₂), the most active compound in previous in vitro tests, also reported for comparisons. It is worth mentioning that, in order to obtain comparable biological tests, log GI₅₀ in Table 3 were all measured in the same experiment. The percent of growth and the inhibition exerted by different doses (0.01–100 μ M) are recorded in Figure 2. In addition to anti-proliferative effects (log GI₅₀), all the derivatives exhibit a significant cytotoxic activity, expressed as logLC₅₀ values; in particular compound 1h shows the best value of both log GI₅₀ and logLC₅₀.

Figure 3 reports the experimental activity values for the new structures (yellow points) and for the test set (black points) versus those predicted by the ten structures model. Experimental values for the designed compounds are even higher than the predicted ones confirming the validity of the Volsurf approach and that the presence of three aromatic moieties and of halogen atoms are the main structural features which determine an increase in the antiproliferative activities.

3. Experimental

3.1. Computational methods

3.1.1. VolSurf+ descriptors. The interaction of molecules with biological membranes is mediated by surface properties such as shape, electrostatic forces, H-bonds and hydrophobicity. Therefore, the GRID¹⁶ force field was chosen to characterize potential polar and hydrophobic interaction sites around target molecules by the water (OH2), the hydrophobic (DRY), and the carbonyl oxygen (O) and amide nitrogen (N1) probe. The information contained in the MIF is transformed into a quantitative scale by calculating the volume or the surface of the interaction contours. The VolSurf+ procedure is as follows: (i) in the first step, the 3D molecular field is generated from the interactions of the OH₂, the DRY, O and N1 probe

Table 3. In vitro antitumour activities, expressed as log GI₅₀, for MCF7 cell line

Compounds/ cell line	3c	1f	2f	3f	1e	2e	3e	1h	2h	1i	1j	1k	2k	3k	3l	1m	PF ₂
MCF7	-5.50	-6.66	-6.20	-6.90	-6.87	-5.76	-7.24	-7.42	-6.72	-6.90	-6.42	-7.18	-6.65	-6.72	-5.76	-6.48	-5.60

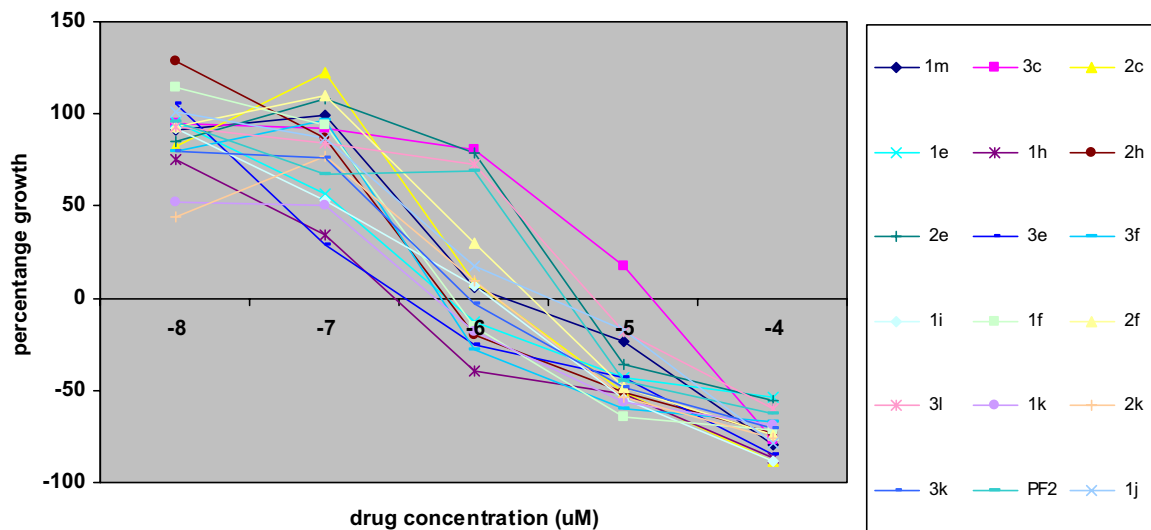


Figure 2. Dose–response curves of antiproliferative activities versus MCF7.

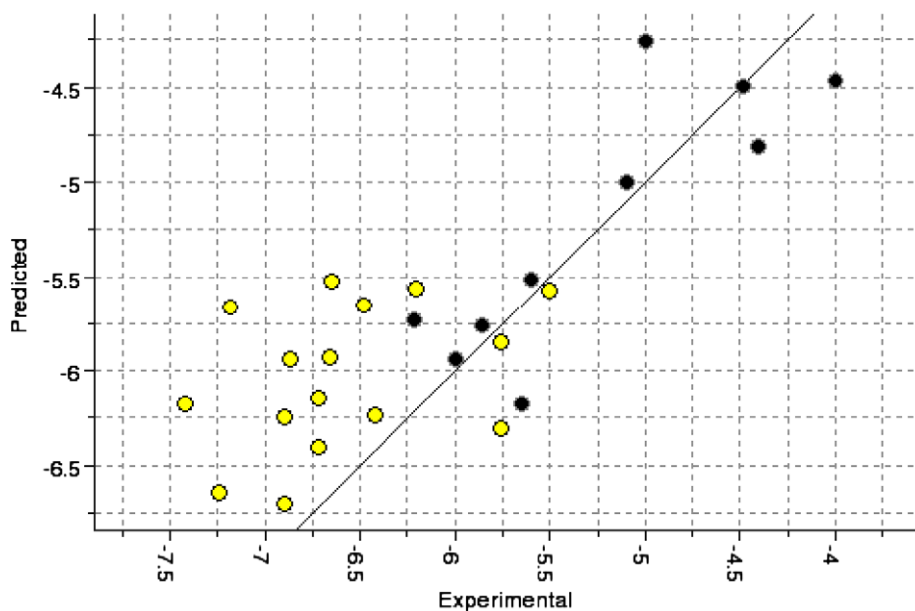


Figure 3. Experimental against predicted values for the new structures (yellow) and for the test set (black).

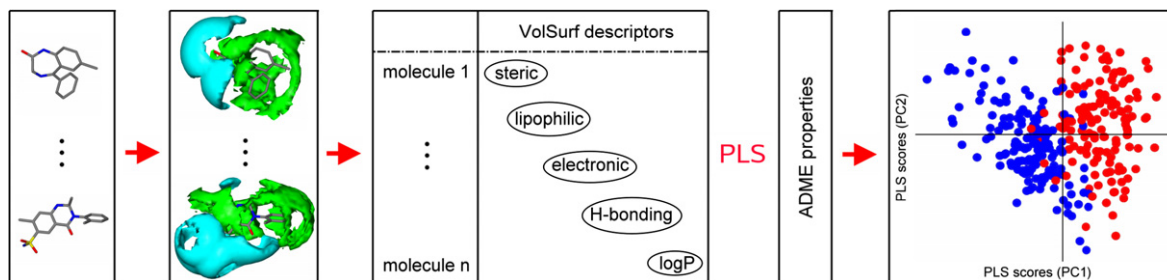


Figure 4. The sequence of steps in chemometric analyses using VolSurf+ descriptors is summarized.

around a target molecule; (ii) the second step consists in the calculation of descriptors from the 3D maps obtained in the first step. The molecular descriptors

obtained, called VolSurf+ descriptors, refer to molecular size and shape, to hydrophilic and hydrophobic regions and to the balance between them, to molecu-

lar diffusion, $\log P$, $\log D$, to the ‘charge state’ descriptors, to the new 3D pharmacophoric descriptors and to some descriptors on some relevant ADME properties. The definition of all 126 VolSurf+ descriptors is given in^{17–21} (case studies with the old versions of VolSurf) and reported in detail in Table 1; (iii) finally, chemometric tools (PCA,²² PLS²³) are used to create relationships of the VolSurf+ descriptor matrix with ADME properties. A scheme of the VolSurf+ program steps is reported in Figure 4. For the detailed definition of Volsurf+ descriptors, see Table 4.

3.2. Compounds

Heteroaromatic carboxaldehydes were Aldrich commercial products.

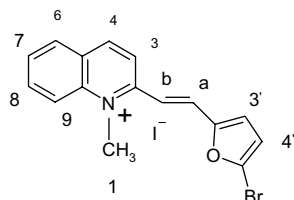
¹H NMR spectra were recorded on a Varian^{Unity Inova} spectrometer operating at 500 MHz, at 25 °C in (CD₃)₂SO using TMS or acetone (2.225 ppm) as internal standards. The spectral width was set to 5000 Hz, with an excitation pulse of 60°, an acquisition time of 3.5 s and a digital resolution after zero-filling of 0.15 Hz/pt.

Electron Spray Ionisation mass spectra were recorded on a Thermo Finnigan LCQ Deca mass spectrometer equipped with an ESI source.

2-Heteroaryl furan derivatives, all iodide salts, were obtained by refluxing in ethanol equimolar amounts of 1,2,3-trimethylimidazolium iodide, or 1,2-dimethylpicolinium iodide or 1,2-dimethyl quinolinium iodide and the appropriate heteroaromatic aldehyde in the presence of few drops of 20% NaOH. The resulting precipitate was recrystallized from ethanol.

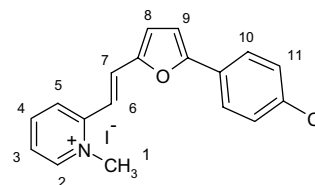
Details on the synthetic conditions and products characterization are reported below:

3.2.1. *trans* 2-[2-(5-bromo-furan-2-yl)vinyl]-1-methylquinolinium iodide (3c).



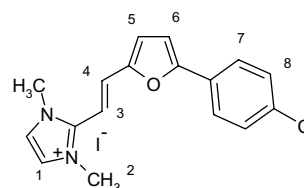
From 5-bromo-furan aldehyde (0.098 g, 0.560 mmol) and 1,2-dimethylquinolinium iodide (0.15 g, 0.560 mmol), 3 ml ethanol, one drop NaOH. The solution was refluxed for two hours. Green needles (68 mg, 29%); mp 210 °C; δ_{H} (500 MHz; DMSO-*d*₆, TMS): 8.03 (d, 1H, $J = 16$ Hz, Ha), 7.53 (d, 1H, $J = 15.5$ Hz, Hb), 4.51 (s, 3H, H₁), 8.34 (d, 1H, $J = 7$ Hz, H₃), 8.54 (d, 1H, $J = 9$ Hz, H₄), 8.48 (d, 1H, $J = 9$ Hz, H₆), 7.94 (t, 1H, $J = 8$ Hz, H₇), 8.17 (t, 1H, $J = 7$ Hz, H₈), 9.03 (d, 1H, $J = 9$ Hz, H₉), 7.24 (d, 1H, $J = 3.5$ Hz, H_{3'}), 6.94 (d, 1H, $J = 3.5$ Hz, H_{4'}); MS: M⁺ Br₇₉ = 314.2; M⁺ Br₈₁ = 316.2.

3.2.2. *trans* 2-[2-[5-(4-Chlorophenyl)furan-2-yl]vinyl]-1-methylpyridinium iodide (1f).



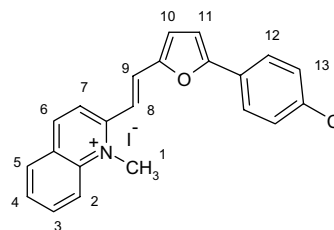
From 1,2-Dimethylpyridinium iodide (176.3 mg, 0.750 mmol) and 5-(4-chlorophenyl)furfural (155.0 mg, 0.750 mmol) in 4 ml ethanol at rt; the mixture was stirred for 30 min. Orange solid (257.0 mg, 80.9%); mp 249–251 °C; δ_{H} (500 MHz; DMSO-*d*₆, TMS): 4.39 (s, 3H, H₁), 7.18 (d, 1H $J = 3.5$ Hz, H₈), 7.31 (d, 1H, $J = 3.5$ Hz, H₉), 7.38 (d, 1H, $J = 15.5$ Hz, H₆), 7.57 (d, 2H, $J = 9$ Hz, H₁₀), 7.86 (t, 1H, $J = 6.5$ Hz, H₃), 7.88 (d, 1H, $J = 16$ Hz, H₇), 7.97 (d, 2H, $J = 9$ Hz, H₁₁), 8.44–8.50 (m, 2H, H_{4/5}), 8.88 (d, 1H, $J = 6.5$ Hz, H₂); MS: M⁺ Cl₃₅ = 296.3, M⁺ Cl₃₇ = 298.3.

3.2.3. *trans* 2-[2-[5-(4-Chlorophenyl)furan-2-yl]vinyl]-1,3-dimethylimidazolium iodide (2f).



From 1,2,3-Trimethylimidazolium iodide (178.6 mg, 0.750 mmol) and 5-(4-chlorophenyl)furfural (155.0 mg, 0.750 mmol) in 4 ml ethanol at rt; the mixture was stirred for 3 d. Yellow solid (110.6 mg, 34.6%); mp 263–265 °C; δ_{H} (500 MHz; DMSO-*d*₆, TMS): 3.94 (s, 6H, H₂), 7.06 (d, 1H, $J = 16$ Hz, H₃), 7.08 (d, 1H, $J = 3$ Hz, H₅), 7.26 (d, 1H, $J = 3.5$ Hz, H₆), 7.47 (d, 1H, $J = 16.5$ Hz, H₄), 7.56 (d(sex), 1H, $J = 8.5$ Hz, H₇), 7.74 (s, 2H, H₁), 7.94 (d(sex), 1H, $J = 8.5$ Hz, H₈); MS: M⁺ Cl₃₅ = 299.3, M⁺ Cl₃₇ = 301.3.

3.2.4. *trans* 2-[2-[5-(4-Chlorophenyl)furan-2-yl]vinyl]-1-methylquinolinium iodide (3f).



From 1,2-Dimethylquinolinium iodide (213.8 mg, 0.750 mmol) and 5-(4-chlorophenyl)furfural (155.0 mg, 0.750 mmol) in 4 ml ethanol at rt; the mixture was stirred for 45 min. Red-brown solid (243.8 mg, 68.7%); mp 224–226 °C; δ_{H} (500 MHz; DMSO-*d*₆, TMS): 4.57 (s, 3H, H₁), 7.34 (d, 1H, $J = 4$ Hz, H₁₀), 7.39 (d, 1H, $J = 4$ Hz, H₁₁), 7.60 (d(sex), 2H, $J = 8.5$ Hz, H₁₂), 7.71 (d, 1H, $J = 15.5$ Hz, H₉), 7.94 (t, 1H, $J = 7.25$ Hz, H₄), 8.04 (d(sex), 2H, $J = 9$ Hz, H₁₃), 8.16 (d, 1H,

Table 4. Detailed definition of Volsurf+ descriptors

	Size and shape descriptors
Molecular volume (V)	represents the water-excluded volume (in Å ³), i.e. the volume enclosed by the water-accessible surface computed at a repulsive value of +0.2 kcal/mol.
Molecular surface (S)	represents the accessible surface (in Å ²) traced out by a water probe interacting at +0.2 kcal/mol when a water molecule rolls over the target molecule.
Rugosity (R)	is a measure of molecular wrinkled surface; it represents the ratio of volume/surface. The smaller the ratio, the larger the rugosity.
Molecular globularity (G)	is defined as S/S_{equiv} with S_{equiv} = surface area of a sphere of volume V, where S and V are the molecular surface and volume described above, respectively. Globularity is 1.0 for perfect spherical molecules. It assumes values greater than 1.0 for real spheroidal molecules. Globularity is also related to molecular flexibility.
Flexibility parameters (Flex, Flex_RB)	The Flex descriptor represents the maximum flexibility of a molecule. It is the result of the average of the differences between the maximum and minimum distance of every atom with the others searched on 50 random conformers). Flex_RB descriptor is the ratio between Flex and the number of rotatable bonds.
	Descriptors of hydrophilic regions
Hydrophilic volumes (W1 - W8)	describe the molecular envelope which is accessible to and attractively interacts with water molecules. The volume of this envelope varies with the level of interaction energies. Hydrophilic descriptors computed from molecular fields of -0.2 to -1.0 kcal/mol account for polarizability and dispersion forces; descriptors from molecular fields of -1.0 to -6.0 kcal/mol account for polar and H-bond donor-acceptor regions.
Capacity factors(CW1 - CW8)	represent the ratio of the hydrophilic surface over the total molecular surface. In other words, it is the hydrophilic surface per surface unit. Capacity factors are calculated at eight different energy levels, the same levels used to compute the hydrophilic volumes.
	Descriptors of hydrophobic regions
Hydrophobic volumes (D1–D8)	GRID ^a uses a probe called DRY to generate 3D lipophilic fields. In analogy to hydrophilic regions, hydrophobic regions may be defined as the molecular envelope generating attractive hydrophobic interactions. VolSurf computes <i>hydrophobic descriptors</i> at eight different energy levels adapted to the usual energy range of hydrophobic interactions (from -0.2 to -1.6 kcal/mol).
Capacity factors(CD1 - CD8)	represent the ratio of the hydrophobic surface over the total molecular surface. In other words, it is the hydrophobic surface per surface unit. Capacity factors are calculated at eight different energy levels, the same levels used to compute the hydrophobic volumes.
Differences of the Hydrophobic volumes (DD1 - DD8)	The difference between the maximum conformational hydrophobic volumes and the hydrophobic volumes (D1–D8) of the the imported 3D structure calculated at the eight levels of energy.
	INTERaction energy (= INTEGy) moments
INTEGY moments (IW1 - IW4, ID1 - ID4)	express the unbalance between the centre of mass of a molecule and the barycentre of its hydrophilic or hydrophobic regions. When referring to hydrophilic regions, integrity moments (IW1-IW4) are vectors pointing from the centre of mass to the centre of the hydrophilic regions: high integrity moments indicate a clear concentration of hydrated regions in only one part of the molecular surface, small indicate that the polar moieties are either close to the centre of mass or they balance at opposite ends of the molecule, so that their resulting barycentre is close to the centre of the molecule. When referring to hydrophobic regions, integrity moments measure the unbalance between the centre of mass of a molecule and the barycentre of the hydrophobic regions.
	Descriptors of H-bond donor / acceptor regions
H-bond donor volumes (WO1 - WO6)	GRID ^a uses a probe called O (carbonylic oxygen) to generate 3D H-bond donor fields. In analogy to hydrophilic regions, H-bond donor regions may be defined as the molecular envelope generating attractive H-donor interactions. VolSurf computes <i>H-bond donor descriptors</i> at six different energy levels adapted to the usual energy range of interactions (from -1 to -6 kcal/mol).
H-bond acceptor volumes (WN1 - WN6)	GRID ¹⁵ uses a probe called N1 (amide nitrogen) to generate 3D H-bond acceptor fields. In analogy to H-bond donor regions, H-bond acceptor volumes may be defined as the molecular envelope generating attractive H-bond acceptor interactions. VolSurf+ computes <i>H-bond acceptor descriptors</i> at six different energy levels adapted to the usual energy range of interactions (from -1 to -6 kcal/mol).
	Mixed descriptors
Hydrophilic-Lipophilic balance (HL1, HL2)	It is the ratio between the hydrophilic regions measured at -3 and -4 kcal/mol and the hydrophobic regions measured at -0.6 and -0.8 kcal/mol. The balance describes which effect dominates in the molecule, or if they are roughly equally balanced.
Amphiphilic moments (A)	is defined as a vector pointing from the centre of the hydrophobic domain to the centre of the hydrophilic domain. The vector length is proportional to the strength of the amphiphilic moment, and it may determine the ability of a compound to permeate a membrane.
Critical packing parameter(CP)	defines a ratio between the hydrophilic and lipophilic part of a molecule. In contrast to the hydrophilic-lipophilic balance, critical packing refers just to molecular shape. It is defined as: $\text{volume}(\text{lipophilic part}) / [(\text{surface}(\text{hydrophilic part}))(\text{length of lipophilic part})]$ Lipophilic and hydrophilic calculations are performed at -0.6 and -3.0 kcal/mol, respectively. Critical packing is a good parameter to predict molecular packing such as in micelle formation, and may be relevant in solubility studies in which the melting point plays an important role.
Polarizability (POL)	is not computed from 3D-molecular fields. Polarizability is an estimate of the average molecular polarizability, calculated according to Miller. ²⁵ This method is based on the structure of the compounds (and not any molecular field) and is therefore independent of the number and type of probes used. The correlation between the experimental molecular polarizability and the polarizability calculated with VolSurf for more than 300 chemicals is very good ($r = 0.99$).
Diffusivity (DIFF)	computed using a modified Stokes–Einstein equation controls the dispersion of chemical in water fluid.
Molecular weight (MW)	is simply computed by summing the atomic weights.
Log P 1-octanol/water (LOGP n-Oct)	The logarithm of the partition coefficient between 1-octanol and water is computed via a linear equation derived by fitting GRID-derived atom type to experimental data on <i>n</i> -octanol/water partition coefficients.
Log P cyclohexane/water (LOGP c-Hex)	The logarithm of the partition coefficient between cyclohexane and water is computed via a linear equation derived by fitting GRID-derived atom types to experimental data on cyclohexane/water partition coefficients.

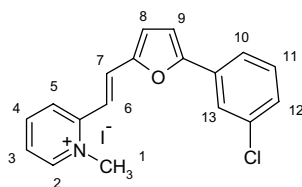
(continued on next page)

Table 4 (continued)

LogD (LgD5 - LgD10)	The logarithm of the coefficient of diffusion between 1-octanol and water is computed via the sum of the logP and the fraction of every species at pH 5, 6, 7, 7.5, 8, 9 and 10.
Polar and Hydrophobic Surface Areas (PSA, HSA, PSAR, PHSAR)	The Polar Surface Area (PSA) is calculated via the sum of polar GRID atom types contributions, while the Hydrophobic Surface Area is calculated via the sum of hydrophobic GRID atom types contributions. PSAR is the ratio between the polar surface area (PSA) and the Surface (S), while PHSAR is the ratio between the polar surface area (PSA) and the hydrophobic surface area (HSA).
Number of Charged Centers (NCC)	Charge State descriptors It reports the number of charged centres present in the imported molecule, according to its charge state at the chosen pH.
Available Uncharged Species (AUS7.4)	This parameter represent the available uncharged species at pH 7.4 and it is calculated as the logarithm of the percentage of the unionised species at pH 7.4 + 2 (AUS7.4 = log(% unionised) + 2).
% Unionised species (%FU4 - %FU10)	The percentage of unionised species is calculated at pH 4, 5, 6, 7, 8, 9 and 10.
Dry, H-bond donor, H-bond acceptor and mixed Dry, H-bond donor and acceptor 3D-triplet pharmacophoric areas (DRDRDR, DRDRAC, DRDRDO, DRACAC, DRACDO, DRDODO, ACACAC, ACACDO, ACDODO, DODODO)	3D pharmacophoric descriptors (TOPP) These parameters represent 3D pharmacophoric descriptors based on the TOPP (Triplets Of Pharmacophoric Points) descriptors. At first the atoms (points) of a structure are classified as Dry, H-bond donor and H-bond acceptor, then all possible triplet of distances between these atoms are generated. The VolSurf+ 3D pharmacophoric descriptors are the maximum conformational area of the triangles derived from every following class of pharmacophoric triplets: DRDRDR refers to the Dry-Dry-Dry triplet, DRDRAC refers to the Dry-Dry-Acceptor triplet, DRDRDO refers to the Dry-Dry-Donor triplet, DRACAC refers to the Dry-Acceptor-Acceptor triplet, DRACDO refers to the Dry-Acceptor-Donor triplet, DRDODO refers to the Dry-Donor-Donor triplet, ACACAC refers to the Acceptor-Acceptor-Acceptor triplet, ACACDO refers to the Acceptor-Acceptor-Donor triplet, ACDODO refers to the Acceptor-Donor-Donor triplet, DODODO refers to the Donor-Donor-Donor triplet.
Intrinsic solubility (SOLY)	ADME model descriptors is computed via a linear equation derived by fitting VolSurf+ descriptors to the logarithm of experimental intrinsic solubility (mole/Litre).
Solubility at various pH (LgS3 - LgS11)	They represent the logarithm of solubilities computed at various pHs starting from the intrinsic solubility (mole/Litre). (the used pH values are 3, 4, 5, 6, 7, 7.5, 8, 9, 10, 11).
Solubility profiling coefficients (L0lgS - L4lgS)	These coefficients represent how much the pH-dependent solubility profile is closer to be correlated by Legendre polynomials of grade 0, 1, 2, 3 and 4, respectively. These parameters are useful to distinguish compounds that present similar solubility but different pH-dependent profile or vice versa, like in the presence of bases, acids, zwitterions or multiprotic compounds.
CACO2 permeability (CACO2)	is computed via a linear equation derived by fitting VolSurf+ descriptors to experimental data on CACO2 cells permeability.
Skin permeability (SKIN)	is computed via a linear equation derived by fitting VolSurf+ descriptors to experimental data on skin permeability.
% of protein binding (PB)	is computed via a linear equation derived by fitting VolSurf+ descriptors to experimental data on percentage of protein binding.
Volume of Distribution (VD)	is computed via a linear equation derived by fitting VolSurf+ descriptors to -log of experimental data on volume of distribution (Litre/Kg).
High Throughput Screening Flag (HTSFlag)	This parameter has value 0 as default. It is active (the value is set to 1) when three of the following conditions of the descriptors are satisfied: D3 > 80; LOGP > 5; PB > 99; SOLY > -6 and CD2 > 0.28.

$J = 15.5$ Hz, H_8), 8.18 (t(sex), 1H, $J = 7.75$ Hz, H_3), 8.33 (d(quar), 1H, $J = 8.25$ Hz, H_7), 8.54 (d, 1H, $J = 9$ Hz, H_5), 8.54 (d, 1H, $J = 10$ Hz, H_6), 9.01 (d, 1H, $J = 9$ Hz, H_2); MS: $M^+ Cl_{35} = 346.3$, $M^+ Cl_{37} = 348.3$.

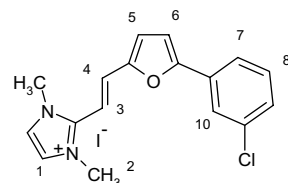
3.2.5. *trans* 2-[2-[5-(3-Chlorophenyl)furan-2-yl]vinyl]-1-methylpyridinium iodide (1e).



From 1,2-Dimethylpyridinium iodide (176.3 mg, 0.750 mmol) and 5-(3-chlorophenyl)furfural (155.0 mg, 0.750 mmol) in 4 ml ethanol at rt; the mixture was stirred for 30 min. Orange needle-shaped solid (221.5 mg, 69.7%); mp 208–210 °C; δ_H (500 MHz; DMSO- d_6 , TMS): 4.40 (s, 3H, H_1), 7.18 (d, 1H, $J = 3.5$ Hz, H_8), 7.39 (d, 1H, $J = 3$ Hz, H_6), 7.42 (d, 1H, $J = 16$ Hz, H_6), 7.46 (d/m, 1H, $J = 8$ Hz, H_{12}), 7.54 (t, 1H, $J = 8$ Hz, H_{11}),

7.87 (t, 1H, $J = 6.5$ Hz, H_3), 7.88 (d, 1H, $J = 15.5$ Hz, H_7), 7.92 (d, 1H, $J = 7.5$ Hz, H_{10}), 8.02 (s/t, 1H, $J = 1.75$ Hz, H_{13}), 8.45–8.50 (m, 2H, $H_{4/5}$), 8.89 (d, 1H, $J = 6.5$ Hz, H_2); MS: $M^+ Cl_{35} = 296.3$, $M^+ Cl_{37} = 298.3$.

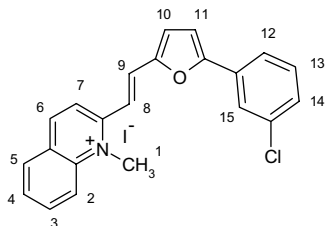
3.2.6. *trans* 2-[2-[5-(3-Chlorophenyl)furan-2-yl]vinyl]-1,3-dimethylimidazolium iodide (2e).



From 1,2,3-Trimethylimidazolium iodide (178.6 mg, 0.750 mmol) and 5-(3-chlorophenyl)furfural (155.0 mg, 0.750 mmol) in 4 ml ethanol at rt; the mixture was stirred for 3 d. Yellow solid (99.4 mg, 31.1%); mp 208–210 °C; δ_H (500 MHz; DMSO- d_6 , TMS): 3.95 (s, 6H, H_2), 7.09 (d, 1H, $J = 3.5$ Hz, H_5), 7.11 (d, 1H, $J = 16$ Hz, H_3), 7.34 (d, 1H, $J = 4$ Hz, H_6), 7.44 (d, 1H, $J = 8$ Hz, H_9), 7.48 (d,

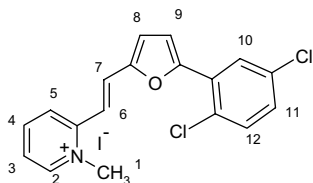
1H, $J = 16.5$ Hz, H₄), 7.52 (d, 1H, $J = 8$ Hz, H₈), 7.75 (s, 2H, H₁), 7.89 (d, 1H, $J = 8$ Hz, H₇), 7.99 (d, 1H, $J = 3.75$ Hz, H₁₀); MS: $M^+ Cl_{35} = 299.3$, $M^+ Cl_{37} = 301.3$.

3.2.7. *trans* 2-[2-[5-(3-Chlorophenyl)furan-2-yl]vinyl]-1-methylquinolinium iodide (3e).



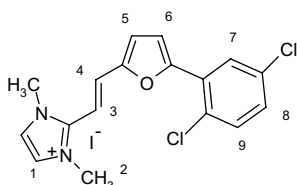
From 1,2-Dimethylquinolinium iodide (213.8 mg, 0.750 mmol) and 5-(3-chlorophenyl)furfural (155.0 mg, 0.750 mmol) in 4 ml ethanol at rt; the mixture was stirred for 40 min. Red-brown solid (117.6 mg, 33.1%); mp 212–214 °C; δ_H (500 MHz; DMSO-*d*₆, TMS): 4.58 (s, 3H, H₁), 7.34 (d, 1H, $J = 3.5$ Hz, H₁₀), 7.46 (d, 1H, $J = 4$ Hz, H₁₁), 7.49 (d, 1H, $J = 8.5$ Hz, H₁₄), 7.56 (t, 1H, $J = 8$ Hz, H₁₃), 7.75 (d, 1H, $J = 15.5$ Hz, H₉), 7.95 (t, 1H, $J = 7.5$ Hz, H₄), 7.99 (d, 1H, $J = 8$ Hz, H₁₂), 8.10 (s/t, 1H, $J = 1.75$ Hz, H₁₅), 8.16 (d, 1H, $J = 16$ Hz, H₈), 8.18 (t/m, 1H, $J = 8$ Hz, H₃), 8.34 (d, 1H, $J = 7.25$ Hz, H₇), 8.54 (d, 1H, $J = 9$ Hz, H₅), 8.57 (d, 1H, $J = 9$ Hz, H₆), 9.02 (d, 1H, $J = 9$ Hz, H₂); MS: $M^+ Cl_{35} = 346.3$, $M^+ Cl_{37} = 348.3$.

3.2.8. *trans* 2-[2-[5-(2,5-Dichlorophenyl)furan-2-yl]vinyl]-1-methylpyridinium iodide (1h).



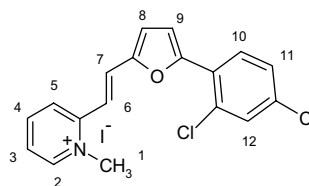
From 1,2-Dimethylpyridinium iodide (0.1763 g, 0.75 mmol) and 5-(2,5-dichlorophenyl)furfural (0.181 mg, 0.75 mmol) in 4 ml ethanol at rt; the mixture was stirred for 30 min. Yellow solid (279.8 mg, 81.5%); mp 235–237 °C; δ_H (500 MHz; DMSO-*d*₆, TMS): 4.40 (s, 3H, H₁), 7.24 (d, 1H, $J = 3.5$ Hz, H₈), 7.48 (d, 1H, $J = 16$ Hz, H₆), 7.48 (d, 1H, $J = 3.5$ Hz, H₉), 7.51 (dd, 1H, $J = 8.5$ Hz, H₁₁), 7.66 (d, 1H, $J = 9$ Hz, H₁₂), 7.89 (d, 1H, $J = 16$ Hz, H₇), 7.89–7.91 (m, 1H, H₃), 8.14 (d, 1H, $J = 2.5$ Hz, H₁₀), 8.48–8.52 (m, 2H, H_{4/5}), 8.92 (d, 1H, $J = 6$ Hz, H₂); MS: $M^+ Cl_{35} = 330.3$, $M^+ Cl_{37} = 332.3$.

3.2.9. *trans* 2-[2-[5-(2,5-Dichlorophenyl)furan-2-yl]vinyl]-1,3-dimethylimidazolium iodide (2h).



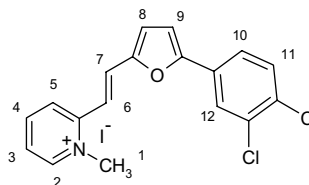
From 1,2,3-Trimethylimidazolium iodide (178.6 mg, 0.750 mmol) and 5-(2,5-dichlorophenyl)furfural (180.8 mg, 0.750 mmol) in 4 ml ethanol at rt; the mixture was stirred for 27 h. Light yellow solid (106 mg, 30.7%); mp 250 °C; δ_H (500 MHz; DMSO-*d*₆, TMS): 3.95 (s, 6H, H₂), 7.16 (d, 1H, $J = 3.5$ Hz, H₅), 7.17 (d, 1H, $J = 16.5$ Hz, H₃), 7.45 (d, 1H, $J = 3.5$ Hz, H₆), 7.49 (dd, 1H, $J = 8.5$ Hz, H₈), 7.51 (d, 1H, $J = 16.5$ Hz, H₄), 7.65 (d, 1H, $J = 9$ Hz, H₉), 7.76 (s, 2H, H₁), 8.12 (d, 1H, $J = 2$ Hz, H₇); MS: $M^+ Cl_{35} = 333.3$, $M^+ Cl_{37} = 335.3$, $M^+ Cl_{37} = 337.2$.

3.2.10. *trans* 2-[2-[5-(2,4-Dichlorophenyl)furan-2-yl]vinyl]-1-methylpyridinium iodide (1i).



From 1,2-Dimethylpyridinium iodide (176.3 mg, 0.750 mmol) and 5-(2,4-dichlorophenyl)furfural (180.8 mg, 0.750 mmol) in 4 ml ethanol at rt; the mixture was stirred for 35 min. Yellow solid (303.4 mg, 88.3%); mp 240–242 °C; δ_H (500 MHz; DMSO-*d*₆, TMS): 4.85 (s, 3H, H₁), 7.65 (d, 1H, $J = 3.5$ Hz, H₈), 7.99 (d, 1H, $J = 16$ Hz, H₆), 7.94 (d, 1H, $J = 3.5$ Hz, H₉), 8.07 (d, 1H, $J = 8.5$ Hz, H₁₀), 8.18 (d, 1H, $J = 15.5$ Hz, H₇), 8.23 (d, 1H, $J = 2$ Hz, H₁₂), 8.31 (t, 1H, $J = 7.25$ Hz, H₃), 8.68 (d, 1H, $J = 9$ Hz, H₁₁), 8.81 (d, 1H, $J = 7$ Hz, H₅), 8.93 (t, 1H, $J = 7.75$ Hz, H₄), 9.08 (d, 1H, $J = 6$ Hz, H₂); MS: $M^+ Cl_{35} = 330.3$, $M^+ Cl_{37} = 332.3$.

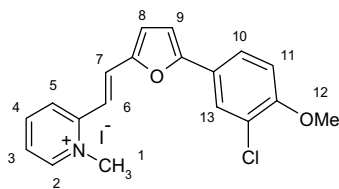
3.2.11. *trans* 2-[2-[5-(3,4-Dichlorophenyl)furan-2-yl]vinyl]-1-methylpyridinium iodide (1j).



From 1,2-Dimethylpyridinium iodide (176.3 mg, 0.750 mmol) and 5-(3,4-dichlorophenyl)furfural (180.8 mg, 0.750 mol) in 4 ml ethanol at rt; the mixture was stirred for 25 min. Orange, needle-shaped solid (290.1 mg, 84.4%); mp 232–234 °C; δ_H (500 MHz; DMSO-*d*₆, TMS): 4.86 (s, 3H, H₁), 7.61 (d, 1H, $J = 3.5$ Hz, H₈), 7.66 (d, 1H, $J = 4$ Hz, H₉), 7.90 (d, 1H, $J = 15.5$ Hz, H₆), 8.17 (d, 1H, $J = 15.5$ Hz, H₇), 8.21 (d, 1H, $J = 8.5$ Hz, H₁₀), 8.30 (t, 1H, $J = 6.75$ Hz, H₃), 8.38 (dd, 1H, $J = 8.5$ Hz, H₁₁), 8.68 (d, 1H, $J = 2$ Hz, H₁₂), 8.81 (d, 1H, $J = 8$ Hz, H₅), 8.92 (d, 1H, $J = 7.25$ Hz, H₄), 9.09 (d, 1H, $J = 6.5$ Hz, H₂); MS: $[M^+ - CH_3] = 330.2$, $M^+ Cl_{35} Cl_{37} = 332.2$.

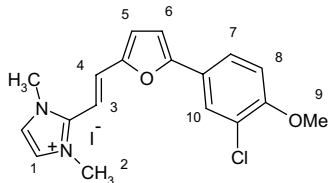
3.2.12. *trans* 2-[2-[5-(3-Chloro-4-methoxyphenyl)furan-2-yl]vinyl]-1-methylpyridinium iodide (1k).

From 1,2-Dimethylpyridinium iodide (176.3 mg, 0.750 mmol) and 5-(3-chloro-4-methoxyphenyl)furfural



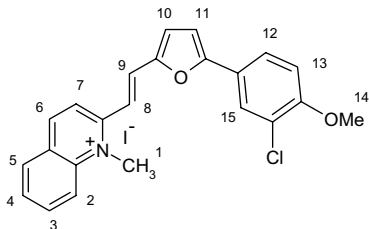
(177.5 mg, 0.750 mmol) in 4ml ethanol at rt; the mixture was stirred for 40 min. Orange solid (315.6 mg, 92.8%); mp 224–226 °C; δ_{H} (500 MHz; DMSO- d_6 , TMS): 3.92 (s, 3H, H₁₂), 4.38 (s, 3H, H₁), 7.15 (d, 1H, $J = 3.5$ Hz, H₈), 7.23 (d, 1H, $J = 3.5$ Hz, H₉), 7.27 (d, 1H, $J = 8.5$ Hz, H₁₁), 7.34 (d, 1H, $J = 16$ Hz, H₆), 7.83 (t, 1H, $J = 6$ Hz, H₃), 7.86 (d, 1H, $J = 15.5$ Hz, H₇), 7.89 (d(quad), 1H, $J = 8.5$ Hz, H₁₀), 8.03 (d, 1H, $J = 2$ Hz, H₁₃), 8.42–8.48 (m, 2H, H_{4/5}), 8.86 (d, 1H, $J = 6.5$ Hz, H₂); MS: [M⁺-CH₃]=331.2, M⁺ Cl₃₅ = 326.2, M⁺ Cl₃₇ = 328.2.

3.2.13. *trans* 2-[2-[5-(3-Chloro-4-methoxyphenyl)furan-2-yl]vinyl]-1,3-dimethylimidazolium iodide (2k).



From 1,2,3-Trimethylimidazolium iodide (178.6 mg, 0.750 mmol) and 5-(3-chloro-4-methoxyphenyl)furfural (177.5 mg, 0.750 mmol) in 4ml ethanol at rt; the mixture was stirred for 5 d. Yellow solid (168.2 mg, 49.1%); mp 252–254 °C; δ_{H} (500 MHz; DMSO- d_6 , TMS): 3.92 (s, 3H, H₉), 3.94 (s, 6H, H₂), 7.04 (d, 1H, $J = 16.5$ Hz, H₃), 7.05 (d, 1H, $J = 3.5$ Hz, H₅), 7.18 (d, 1H, $J = 3.5$ Hz, H₆), 7.26 (d, 1H, $J = 9$ Hz, H₈), 7.43 (d, 1H, $J = 16.5$ Hz, H₄), 7.73 (s, 2H, H₁), 7.86 (dd, 1H, $J = 8.75$ Hz, H₇), 8.00 (d, 1H, $J = 2$ Hz, H₁₀); MS: M⁺ Cl₃₅ = 376.2, M⁺ Cl₃₇ = 378.2.

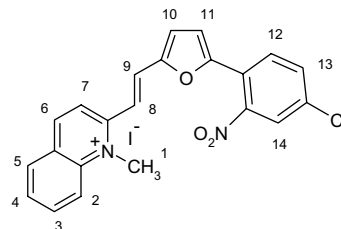
3.2.14. *trans* 2-[2-[5-(3-Chloro-4-methoxyphenyl)furan-2-yl]vinyl]-1-methylquinolinium iodide (3k).



From 1,2-Dimethylquinolinium iodide (213.8 mg, 0.750 mmol) and 5-(3-chloro-4-methoxyphenyl)furfural (177.5 mg, 0.750 mmol) in 4ml ethanol at rt; the mixture was stirred for 60 min. Dark violet solid (236.2 mg, 62.5%); mp 218–220 °C; δ_{H} (500 MHz; DMSO- d_6 , TMS): 3.94 (s, 3H, H₁₄), 4.55 (s, 3H, H₁), 7.29–7.32 (m, 3H, H_{10/11/13}), 7.68 (d, 1H, $J = 15.5$ Hz, H₈), 7.92 (t, 1H, $J = 7.5$ Hz, H₄), 7.97

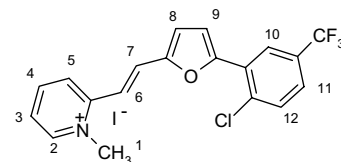
(dd, 1H, $J = 8.75$ Hz, H₁₂), 8.12 (d, 1H, $J = 2.5$ Hz, H₁₅), 8.15 (d, 1H, $J = 15.5$ Hz, H₉), 8.16 (t, 1H, $J = 8$ Hz, H₃), 8.31 (d, 1H, $J = 7.5$ Hz, H₇), 8.52 (d, 1H, $J = 9.5$ Hz, H₅), 8.54 (d, 1H, $J = 8.5$ Hz, H₆), 8.97 (d, 1H, $J = 9$ Hz, H₂); MS: M⁺ Cl₃₅ = 329.2, M⁺ Cl₃₇ = 331.2.

3.2.15. *trans* 2-[2-[5-(4-Chloro-2-nitrophenyl)furan-2-yl]vinyl]-1-methylquinolinium iodide (3l).



From 1,2-Dimethylquinolinium iodide (213.8 mg, 0.750 mmol) and 5-(4-chloro-2-nitrophenyl)furfural (188.7 mg, 0.750 mmol) in 4 ml ethanol at rt; the mixture was stirred for 60 min. Light brown solid (326.1 mg, 83.9%); mp 238–240 °C; δ_{H} (500 MHz; DMSO- d_6 , TMS): 5.02 (s, 3H, H₁), 7.63 (d, 1H, $J = 3.5$ Hz, H₁₀), 7.73 (d, 1H, $J = 3.5$ Hz, H₁₁), 8.03 (d, 1H, $J = 15.5$ Hz, H₈), 8.34 (d, 1H, $J = 15.5$ Hz, H₉), 8.35 (d(quad), 1H, $J = 8$ Hz, H₁₂), 8.48–8.53 (m, 3H, H_{4/13/14}), 8.74 (d, 1H, $J = 7.75$ Hz, H₃), 8.79 (d, 1H, $J = 8.5$ Hz, H₇), 8.82 (d, 1H, $J = 8.5$ Hz, H₅), 8.91 (d, 1H, $J = 9$ Hz, H₆), 9.41 (d, 1H, $J = 8.5$ Hz, H₂); MS: M⁺ Cl₃₅ = 391.2, M⁺ Cl₃₇ = 393.2.

3.2.16. *trans* 2-[2-[5-(2-Chloro-5-trifluoromethylphenyl)furan-2-yl]vinyl]-1-methylpyridinium iodide (1m).



From 5-[2-chloro-5-(trifluoromethyl)phenyl]furan aldehyde (0.425 mmol) and 1,2,3 trimethylimidazolium iodide (0.1008 g, 0.425 mmol), 3 ml ethanol, one drop NaOH. The solution was refluxed for one hour. Yellow needles (83 mg, 39%); mp 237 °C; δ_{H} (500 MHz; DMSO- d_6 , TMS): 4.38 (s, 3H, H₁), 7.30 (d, 1H, $J = 4$ Hz, H₈), 7.47 (d, 1H, $J = 15.5$ Hz, H₆), 7.54 (d, 1H, $^3J = 4$ Hz, H₉), 7.79 (dd, 1H, $J = 8.75$ Hz, H₁₂), 7.88–7.91 (m, 2H, H_{3/11}), 7.91 (d, 1H, $J = 16$ Hz, H₇), 8.31 (s, 1H, H₁₀), 8.47–8.52 (m, 2H, H_{4/5}), 8.91 (d, 1H, $J = 6.5$ Hz, H₂); MS: M⁺ = 364.3.

4. Biological essays

4.1. Human cell line (MCF7)

Human mammary adenocarcinoma (MCF7) were grown in Dulbecco's MEM (DMEM), 1.0 g/l D-glucose. Each medium was supplemented with 10% (vol/vol)

heat-inactivated foetal bovine serum, 2 mM L-Alanyl-L-Glutamine, penicillin–streptomycin (50 U to 50 µg/ml) and incubated at 37 °C in humidified atmosphere of 5% CO₂, 95% air. The culture medium was changed twice a week.

4.2. Treatment with antitumour agents and MTT colorimetric assay

Human cancer cell line (5×10^3 cells/0.33 cm²) was plated in 96-well plates 'Nunclon TM Microwell™' (Nunc) and was incubated at 37 °C. After 24 h, cells were treated with the compounds (final concentration 0.01–100 µM). Untreated cells were used as controls. Microplates were incubated at 37 °C in humidified atmosphere of 5% CO₂, 95% air for 3 days and then cytotoxicity was measured with colorimetric assay based on the use of tetrazolium salt MTT (3-(4,5-dimethylthiazol-2-yl)-2,5-diphenyl tetrazolium bromide).²⁴ The results were read on a multiwell scanning spectrophotometer (Multiscan reader), using a wavelength of 570 nm. Each value was the average of 8 wells (standard deviations were less than 20%). The GI₅₀ value was calculated according to NCI: thus, GI₅₀ is the concentration of test compound where $100 \times (T - T_0)/(C - T_0) = 50$ (T is the optical density of the test well after a 48-h period of exposure to test drug; T_0 is the optical density at time zero; C is the control optical density).

Acknowledgment

We thank the University of Catania for financial support.

References and notes

- Ballistreri, F. P.; Barresi, V.; Benedetti, P.; Caltabiano, G.; Fortuna, C. G.; Longo, M. L.; Musumarra, G. *Bioorg. Med. Chem.* **2004**, *12*, 1689.
- Goodford, P. J. *Med. Chem.* **1985**, *28*, 849.
- Cramer, R. D., III; Patterson, D. E.; Bunce, J. J. *Am. Chem. Soc.* **1988**, *110*, 5959.
- Pastor, M.; Cruciani, G.; McLay, I.; Pickett, S.; Clementi, S. *J. Med. Chem.* **2000**, *43*, 3233.
- González-Díaz, H.; Agüero, G.; Cabrera, M. A.; Molina, R.; Santana, L.; Uriarte, E.; Delogu, G.; Castañedo, N. *Bioorg. Med. Chem. Lett.* **2005**, *15*, 551.
- González-Díaz, H.; Marrero, Y.; Hernandez, I.; Bastida, I.; Tenorio, E.; Nasco, O.; Uriarte, E.; Castanedo, N.; Cabrera, M. A.; Aguila, E.; Marrero, O.; Morales, A.; Perez, M. *Chem. Res. Toxicol.* **2003**, *16*, 1318.
- González-Díaz, H.; Cruz-Monteagudo, M.; Molina, R.; Tenorio, E.; Uriarte, E. *Bioorg. Med. Chem.* **2005**, *13*, 1119.
- Estrada, E. *Mutat Res.* **1998**, *420*, 67.
- González-Díaz, H.; Olazábal, E.; Santana, L.; Uriarte, E.; González-Díaz, Y.; Castañedo, N. *Bioorg. Med. Chem.* **2007**, *15*, 962.
- González-Díaz, H.; Torres-Gómez, L. A.; Guevara, Y.; Almeida, M. S.; Molina, R.; Castañedo, N.; Santana, L.; Uriarte, E. *J. Mol. Model.* **2005**, *11*, 116.
- González-Díaz, H.; Tenorio, E.; Castañedo, N.; Santana, L.; Uriarte, E. *Bioorg. Med. Chem.* **2005**, *13*, 1523.
- González Borroto, J. I.; Pérez Machado, G.; Creus, A.; Marcos, R. *Mutagenesis* **2005**, *20*, 193.
- Cruciani, G.; Pastor, M.; Guba, W. *Eur. J. Pharm. Sci.* **2000**, *11*, S29.
- Doddareddy, M. R.; Cha, J. H.; Cho, Y. S.; Koh, H. Y.; Yoo, K. H.; Kim, D. J.; Pae, A. N. *Bioorg. & Med. Chem.* **2005**, *13*, 3339.
- Fichera, M.; Fortuna, C. G.; Impallomeni, G.; Musumarra, G. *Eur. J. Org. Chem.* **2002**, 145.
- Carosati, E.; Sciabola, S.; Cruciani, G. *J. Med. Chem.* **2004**, *47*, 5114.
- Cruciani, G.; Crivori, P.; Carrupt, P. A.; Testa, B. *J. Mol. Struct.: Theo. Chem.* **2000**, *503*, 17.
- Crivori, P.; Cruciani, G.; Carrupt, P. A.; Testa, B. *J. Med. Chem.* **2000**, *43*, 2204.
- Cruciani, G.; Meniconi, M.; Carosati, E.; Zamora, I.; Mannhold, R.. In *Methods and Principles in Medicinal Chemistry*; van de Waterbeemd, H., Lennernäs, H., Artursson, P., Eds.; Wiley-VCH publishers, 2003; vol. 18, p 406.
- Berellini, G.; Cruciani, G.; Mannhold, R. *J. Med. Chem.* **2005**, *48*, 4389.
- Mannhold, R.; Berellini, G.; Carosati, E.; Benedetti, P.. In *The Molecular Interaction Fields*; Cruciani, G., Mannhold, R., Kubinyi, H., Folkers, G., Eds.; WILEY-VCH Verlag GmbH & Co. KGaA: Weinheim, 2006; vol. 27, p 173.
- S. Wold, M. Sjöström., ed. B.R. Kowalski, 'Chemometrics: Theory and Application,' ed. B.R. Kowalski, ACS Symposium Series, Washington, 1977, 243.
- Wold, S.; Albano, C.; Dunn, W.J. III; Edlund, U.; Esbensen, K.; Geladi, P.; Hellberg, S.; Johansson, E.; Lindberg, W.; Sjöström., M. In 'Chemometrics', ed. B.R. Kowalski, **1984**, 17.
- Mosmann, T. J. *J. Immunol. Meth.* **1983**, *65*, 55.
- Miller, K. J. *J. Am. Chem. Soc.* **1990**, *112*, 8533.